bioRxiv preprint doi: https://doi.org/10.1101/2024.12.06.627202; this version posted December 11, 2024. The copyright holder for this preprint (which was not certified by peer review) is the author/funder, who has granted bioRxiv a license to display the preprint in perpetuity. It is made available under aCC-BY-NC-ND 4.0 International license.

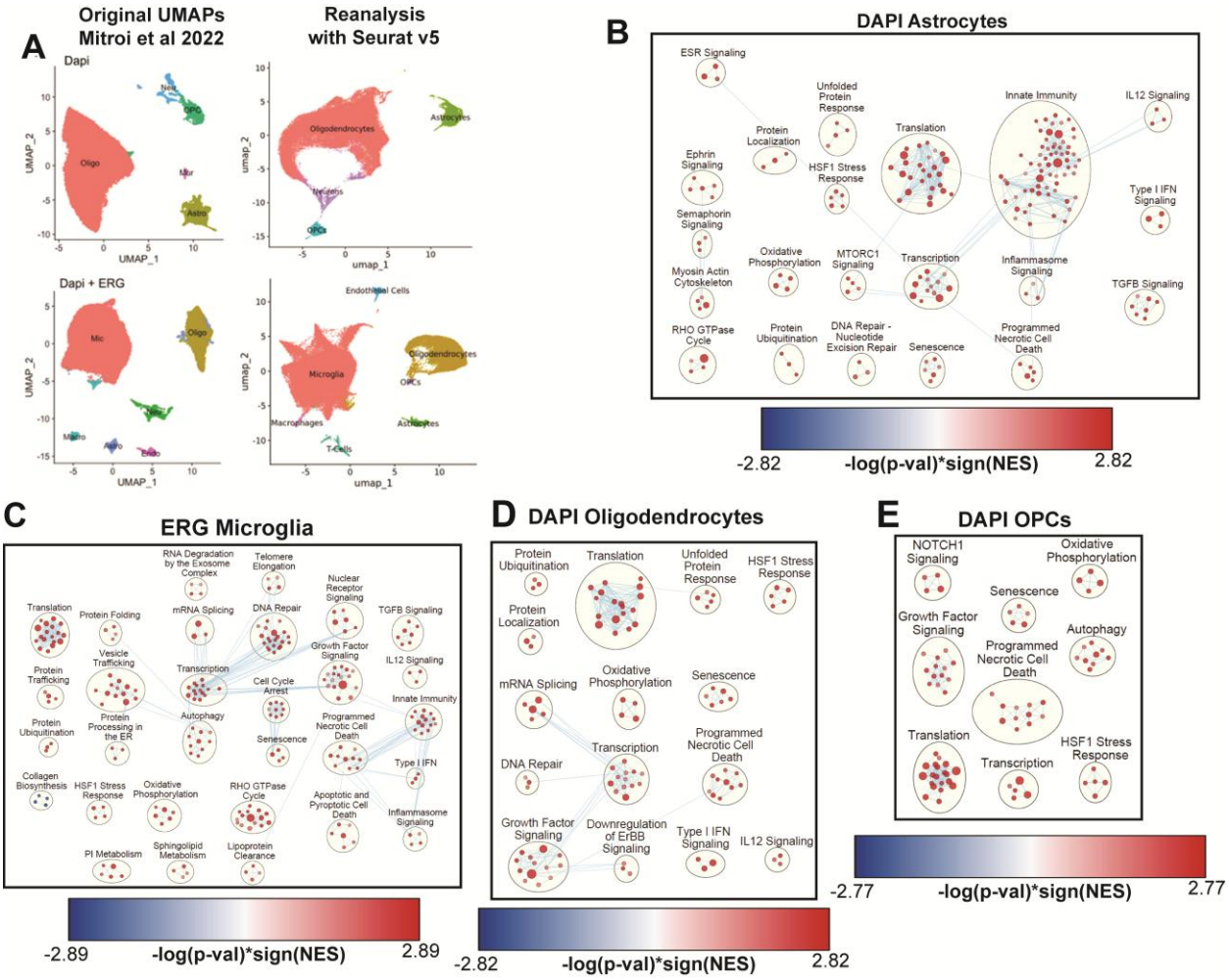

Figure S1 GSEA Analysis of Mitroi et al VaD datasets (**A**) Side by side comparison of Mitroi et al UMAPs from original publication (left) and after reanalysis with our Seurat v5 pipeline (right). (**B-D**) Cytoscape EnrichmentMap showing individual GSEA hits from Reactome (FDR < 0.05) clustered via AutoAnnotate.

bioRxiv preprint doi: https://doi.org/10.1101/2024.12.06.627202; this version posted December 11, 2024. The copyright holder for this preprint (which was not certified by peer review) is the author/funder, who has granted bioRxiv a license to display the preprint in perpetuity. It is made available under aCC-BY-NC-ND 4.0 International license.

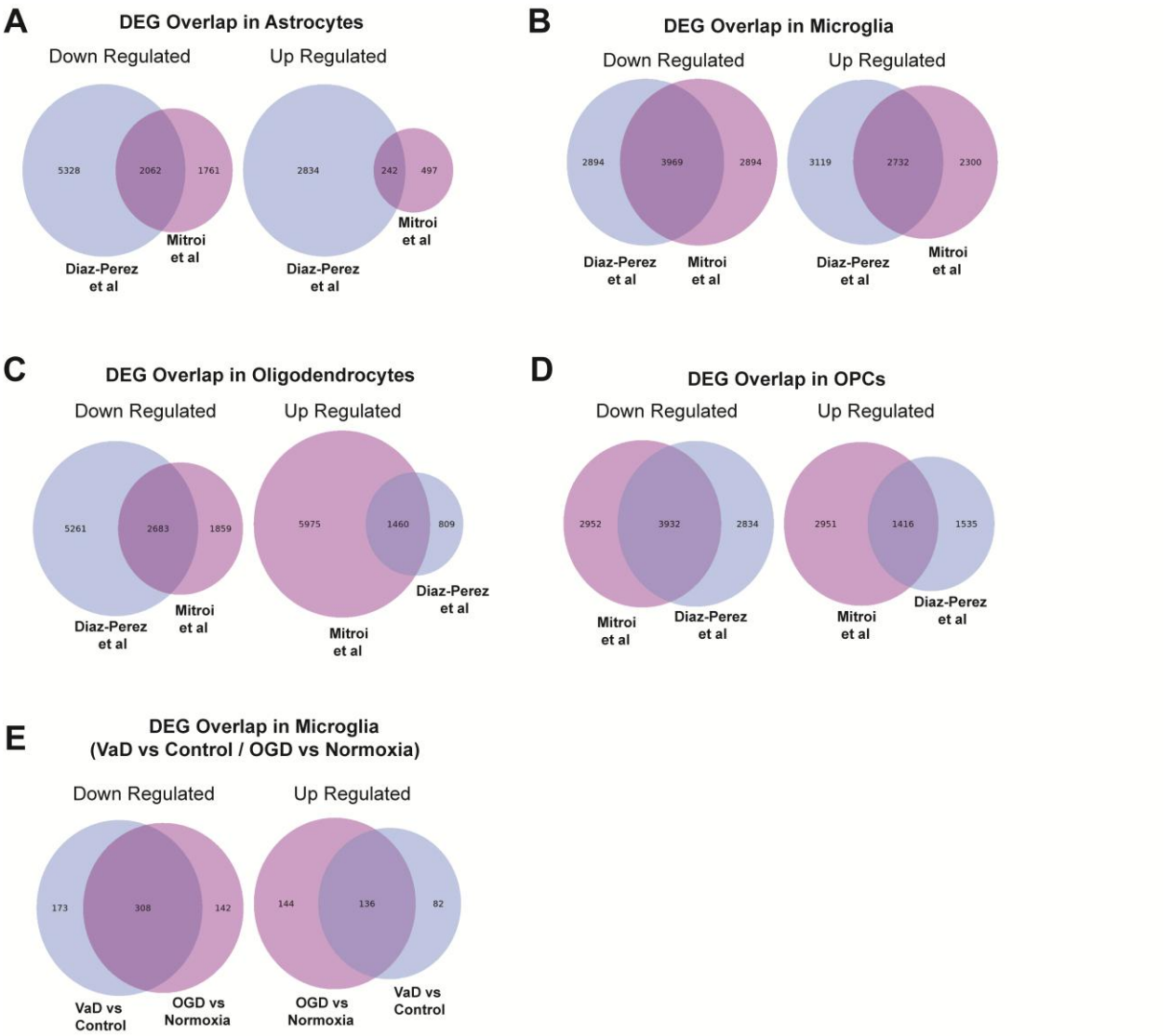

Figure S2 Overlapping genes identified by RRHO in comparisons between transcriptomic datasets Venn diagrams showing overlap of pre-ranked gene lists (VaD vs Control) from (**A**) astrocytes, (**B**) microglia, (**C**) oligodendrocytes and (**D**) OPCs from out dataset (*Diaz-Perez et al*) and the *Mitroi et al* dataset. Venn diagram showing overlap of preranked gene lists between microglia from VaD vs Control and OGD vs Normoxia.

bioRxiv preprint doi: https://doi.org/10.1101/2024.12.06.627202; this version posted December 11, 2024. The copyright holder for this preprint (which was not certified by peer review) is the author/funder, who has granted bioRxiv a license to display the preprint in perpetuity. It is made available under aCC-BY-NC-ND 4.0 International license.

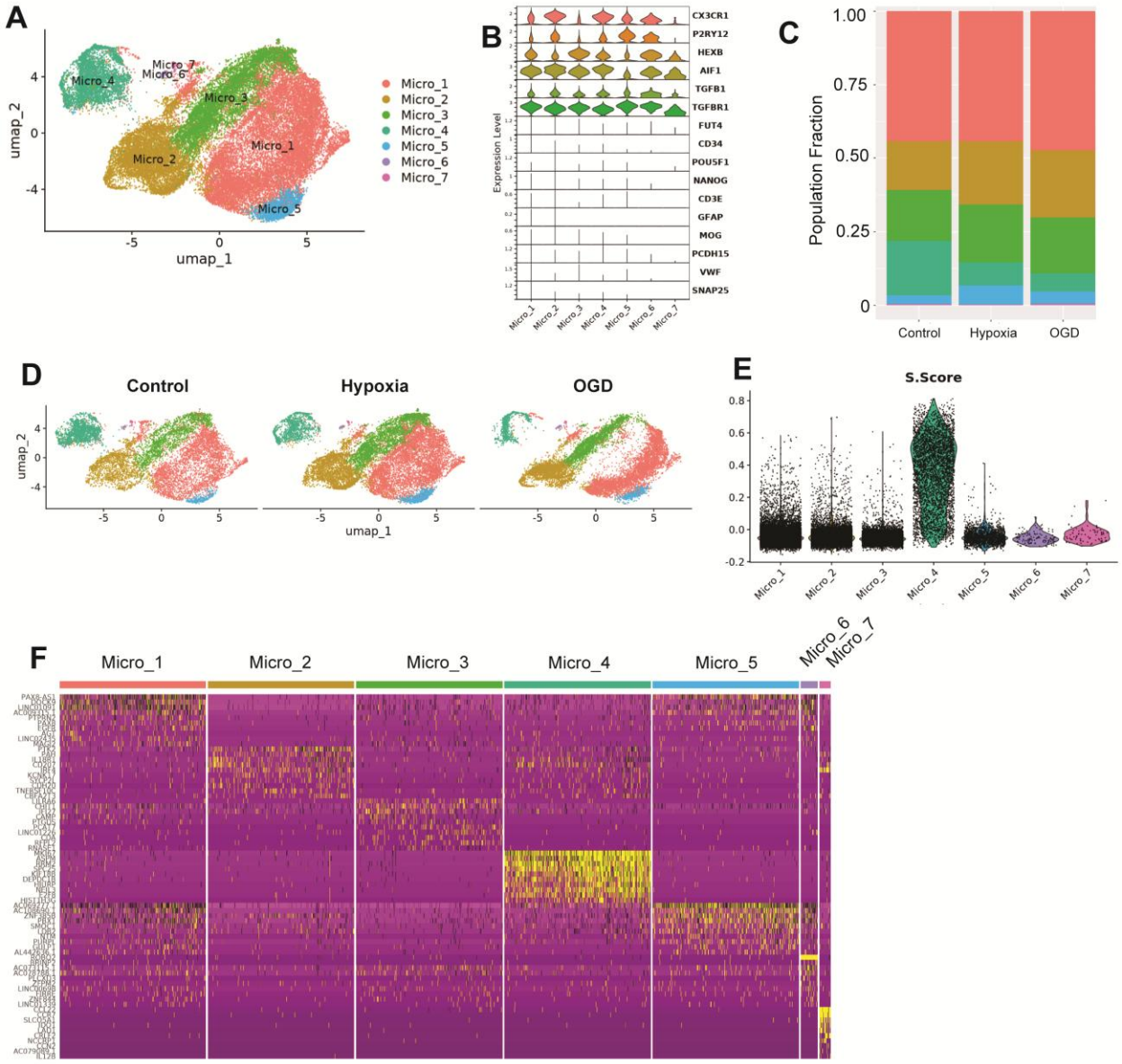

Figure S3 Single cell landscape of iMGL (**A**) UMAP of iMGL dataset. (**B**) Violin plot of multiple microglia-specific, iPSC-specific and other CNS cell type-specific markers in iMGL dataset. (**C**) Cluster proportions split by normoxia, hypoxia and OGD. (**D**) UMAP of iMGL dataset split by normoxia, hypoxia and OGD. (**E**) Module scoring of each cluster using cell cycle genes. (**F**) Heatmap of top 10 markers that distinguish each cluster from all other cells in our dataset.

bioRxiv preprint doi: https://doi.org/10.1101/2024.12.06.627202; this version posted December 11, 2024. The copyright holder for this preprint (which was not certified by peer review) is the author/funder, who has granted bioRxiv a license to display the preprint in perpetuity. It is made available under aCC-BY-NC-ND 4.0 International license.

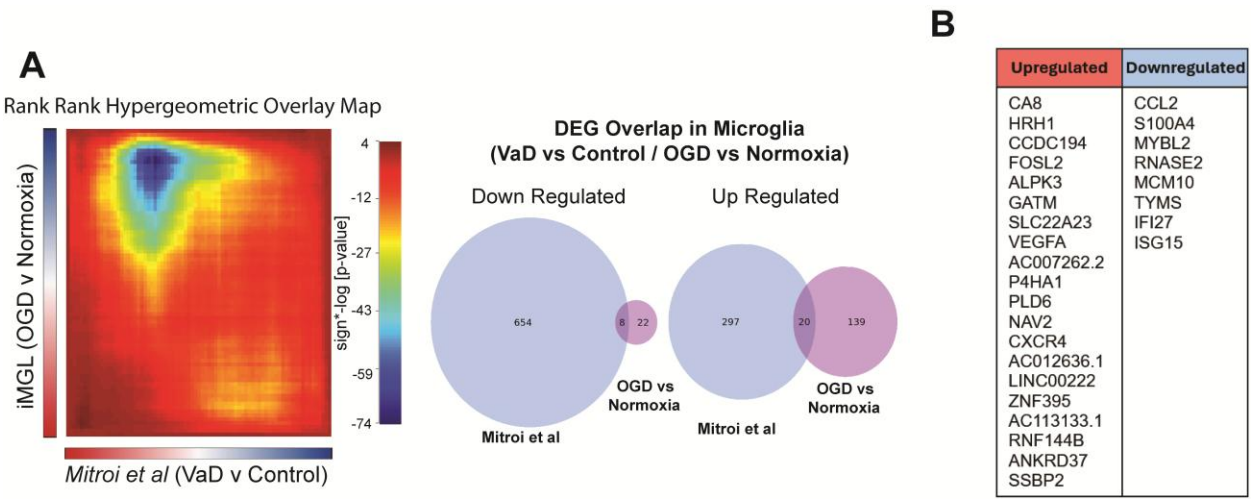

Upregulated	Downregulated
CA8	CCL2
HRH1	S100A4
CCDC194	MYBL2
FOSL2	RNASE2
ALPK3	MCM10
GATM	TYMS
SLC22A23	IFI27
VEGFA	ISG15
AC007262.2	
P4HA1	
PLD6	
NAV2	
CXCR4	
AC012636.1	
LINC00222	
ZNF395	
AC113133.1	
RNF144B	
ANKRD37	
SSBP2	

Figure S4 Anticorrelation of OGD-exposed iMGL and *Mitroi et al* dataset (**A**) RRHO heatmap and Venn diagrams showing overlap of pre-ranked gene lists from *Mitroi et al* (VaD vs Control) and iMGL (OGD vs Normoxia) datasets. Negative values on the -log(p-val) scale is indicative of an almost perfect anti-correlation between the lists of differentially expressed genes from *Mitroi et al* and iMGL. (**B**) List of overlapping upregulated and downregulated genes between *Mitroi et al* and iMGL (no significant hits found on Reactome).

bioRxiv preprint doi: https://doi.org/10.1101/2024.12.06.627202; this version posted December 11, 2024. The copyright holder for this preprint (which was not certified by peer review) is the author/funder, who has granted bioRxiv a license to display the preprint in perpetuity. It is made available under aCC-BY-NC-ND 4.0 International license.

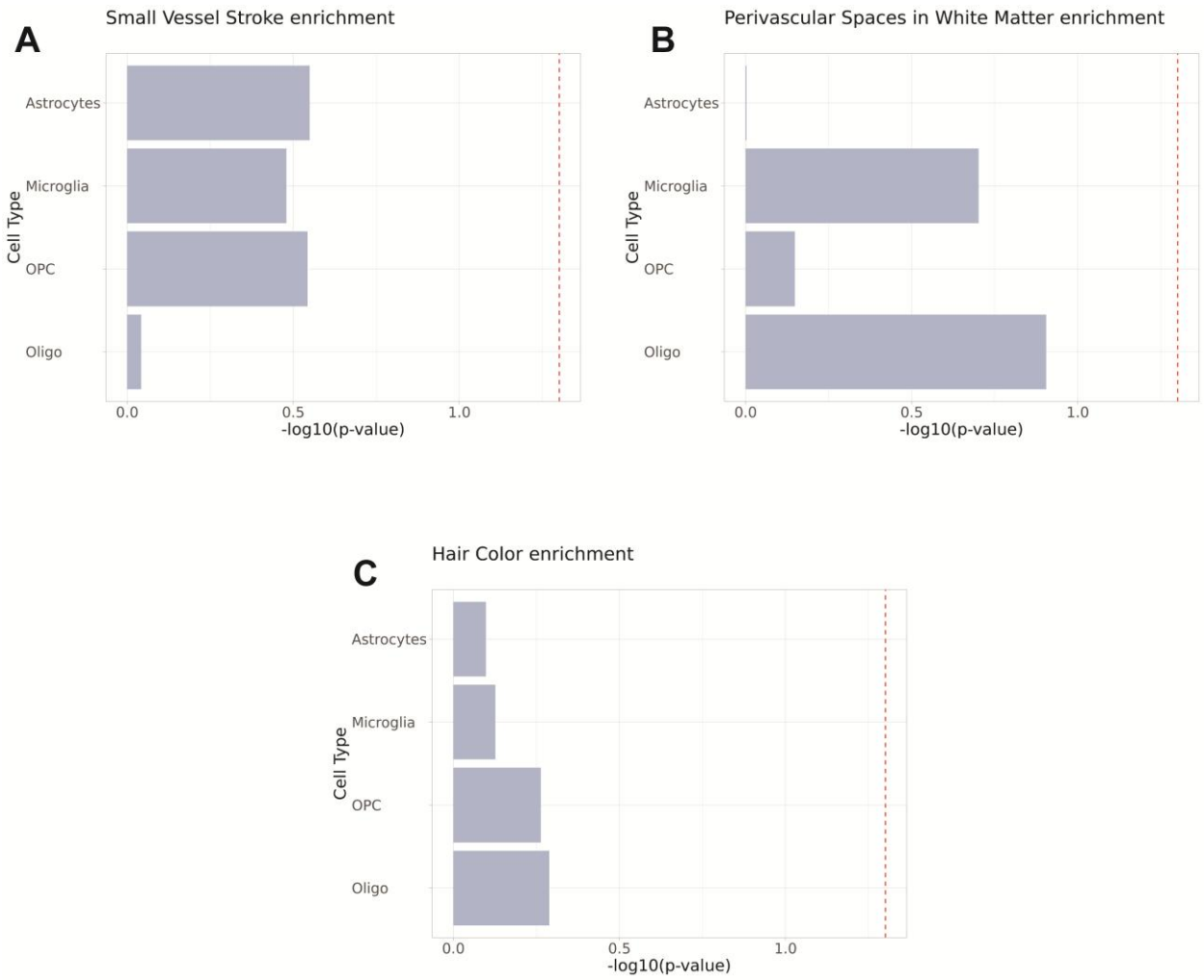

Figure S5 Additional gene-set analysis of GWAS data using MAGMA Association of cell type transcriptomes in VaD with known genetic risk variants linked to (A) small vessel stroke, (B) enlarged perivascular space and (C) hair color (negative control). The red lines represent the p-value threshold of 0.05, indicating statistically significant associations.

bioRxiv preprint doi: https://doi.org/10.1101/2024.12.06.627202; this version posted December 11, 2024. The copyright holder for this preprint (which was not certified by peer review) is the author/funder, who has granted bioRxiv a license to display the preprint in perpetuity. It is made available under aCC-BY-NC-ND 4.0 International license.

Supplemental Table 1. Demographic and histopathological information of periventricular white matter samples

Summarizes the demographic, diagnostic and histopathological information linked to each sample used to generate our single-nucleus RNA sequencing dataset.

Sample Name	Batch	NeuroBioBank ID	Brain Bank	Race	Age	Sex	Cause of Death	Vascular Pathology	Braak & Braak Staging	CAA	PMI (hr)	RIN
Control1	1	S13788	Harvard	White	100	Male	Natural	Mild cSVD with several minute remote microinfarcts	Stage II	No	6.17	7.1
Control2	2	S10213	Harvard	White	86	Female	Natural	Mild cSVD with remote microinfarcts	Stage I	No	6.92	2.3
Control4F	4	S18110	Harvard	White	66	Female	Undetermined	No infarcts or vascular pathology detected.	No neurofibrillary tangles observed.	No	7.42	2.8
Control5	5	S07749	Harvard	Unknown	61	Male	Undetermined	Arteriolosclerosis. Mild edema in cerebral white matter.	Stage I	No	10.08	n/a
VaD1	1	197965	Mt. Sinai	White	98	Female	Bronchopneumonia	Multiple transient ischemic attacks. Extensive cSVD with white matter changes. Large healed cystic infarct from 12 yrs earlier. Area affected was far from sampling area	No neurofibrillary tangles observed.	Unknown	1.83	6.7
VaD2	2	BEB19028	U Miami	White	83	Male	Natural	Hypertensive small vessel disease with non-specific white matter gliosis.	Stage II	No	28.24	8.9
VaD3F	3	S02794	Harvard	White	83	Female	Natural	Extensive cSVD with several microinfarcts in occipital cortex, parietal cortex, anterior commissure, hippocampus and thalamus	Stage I	No	30	5.9
VaD5	5	S02918	Harvard	White	74	Male	Undetermined	Atherosclerosis, arteriosclerosis. Small infarct in left internal capsule (related to prefrontal cortex) and gray matter in pons	Stage I	Yes	13.58	3.1

bioRxiv preprint doi: https://doi.org/10.1101/2024.12.06.627202; this version posted December 11, 2024. The copyright holder for this preprint (which was not certified by peer review) is the author/funder, who has granted bioRxiv a license to display the preprint in perpetuity. It is made available under aCC-BY-NC-ND 4.0 International license.

Supplemental Table 2. Quality Control metrics of sequenced snRNAseq samples

Summarizes the quality control parameters obtained from each sample post-sequencing, after CellRanger alignment and after implementing initial QC cutoffs in Seurat v5.

	Pre-Sequencing		Post-Sequencing Alignment			Dataset Integration				
Name	Ave bp	cDNA (ng/uL)	# of Nuclei	Median Genes per Cell	Total Genes Detected	% Mapped to Transcriptome	Average of MT %	Range of MT %	Pre-Filtering	Post-Filtering	% Filtered
Control1	457	1.48	5,143	2,875	29,657	69.90%	0.80%	0% - 23.09%	5143	4937	4.01%
Control2	515	8.61	3,320	1,826	27,139	62.20%	0.28%	0% - 23.11%	3320	3260	1.81%
Control4F	442	8.61	6,691	2,931	30,872	70.70%	1.33%	0% - 48.44%	6691	6420	4.05%
Control5	469	5.07	2,023	2,159	26,029	36.50%	0.79%	0% - 10.06%	2023	1842	8.95%
VaD1	460	2.22	5,795	2,894	30,179	72.10%	1.73%	0% - 56.07%	5795	5476	5.50%
VaD2	493	22.5	4,784	2,288	29,355	78.00%	0.38%	0% - 35.46%	4784	4374	8.57%
VaD3F	464	3.14	3,287	2,556	30,601	67.30%	1.58%	0% - 74.16%	3287	2670	18.77%
VaD5	469	4.69	5,313	2,457	28,741	63.00%	0.57%	0% - 39.09%	5310	5177	2.50%

bioRxiv preprint doi: https://doi.org/10.1101/2024.12.06.627202; this version posted December 11, 2024. The copyright holder for this preprint (which was not certified by peer review) is the author/funder, who has granted bioRxiv a license to display the preprint in perpetuity. It is made available under aCC-BY-NC-ND 4.0 International license.

Supplemental Table 3. Total number of nuclei contributed by sample

Shows the count of nuclei obtained from each cluster by sample of origin after quality control filtering.

Cluster Annotation	Control1	Control2	Control4	Control5	VaD1	VaD2	VaD3	VaD5
Oligo_1	2511	1835	2677	756	3260	2283	890	2522
Oligo_2	1546	1024	2010	477	1344	1361	591	1392
Astrocytes	162	115	771	170	390	250	292	482
Microglia	364	64	543	60	203	225	155	341
OPCs	107	157	222	173	129	106	231	330
Neurons	161	33	135	164	40	122	423	44
Oligo_3	79	21	30	40	97	24	33	41
Endothelial Cells	7	11	32	2	13	3	55	25

bioRxiv preprint doi: https://doi.org/10.1101/2024.12.06.627202; this version posted December 11, 2024. The copyright holder for this preprint (which was not certified by peer review) is the author/funder, who has granted bioRxiv a license to display the preprint in perpetuity. It is made available under aCC-BY-NC-ND 4.0 International license.

Supplemental Table 4. Correlation of heat shock protein gene expression with post-mortem interval

Shows the Pearson correlation coefficient (R), p-value and adjusted p-value of each gene's expression in relation to increasing post-mortem interval. Comparisons were done with averaged gene expression from whole dataset or by celltype. Adjusted p-value was obtained using the Bonferroni correction.

	Whole Dataset			Astrocytes			Microglia			Oligodendrocytes			OPCs		
Genes	R	p-val	adj p-val	R	p-val	adj p-val	R	p-val	adj p-val	R	p-val	adj p-val	R	p-val	adj p-val
HSPB1	0.54	0.16	1.00	0.58	0.13	1.00	0.23	0.58	1.00	0.47	0.24	1.00	0.46	0.25	1.00
HSP90AA1	0.46	0.26	1.00	0.27	0.51	1.00	-0.02	0.97	1.00	0.55	0.16	1.00	0.72	0.05	0.95
HSP90AB1	0.38	0.36	1.00	0.51	0.20	1.00	-0.05	0.91	1.00	0.39	0.33	1.00	0.52	0.18	1.00
DNAJB6	0.53	0.17	1.00	0.70	0.05	0.95	0.37	0.36	1.00	0.57	0.14	1.00	0.29	0.48	1.00
DNAJB1	0.59	0.13	1.00	0.67	0.07	1.00	-0.10	0.81	1.00	0.64	0.09	1.00	0.49	0.21	1.00
PTGES3	0.49	0.021	0.399	0.65	0.08	1.00	0.39	0.34	1.00	0.54	0.16	1.00	0.58	0.13	1.00
HSPH1	0.54	0.17	1.00	0.55	0.16	1.00	0.23	0.59	1.00	0.58	0.14	1.00	0.63	0.09	1.00
CREBBP	-0.099	0.82	1.00	0.43	0.29	1.00	-0.23	0.58	1.00	0.02	0.96	1.00	-0.02	0.96	1.00
DEDD2	0.52	0.19	1.00	0.41	0.31	1.00	0.09	0.83	1.00	0.54	0.17	1.00	0.69	0.06	1.00
HSPA1A	0.66	0.073	1.00	0.01	0.98	1.00	0.70	0.06	1.00	0.68	0.06	1.00	0.72	0.04	0.76
UBB	0.36	0.38	1.00	0.67	0.07	1.00	0.88	3.59E-03	6.80E-02	0.36	0.38	1.00	0.79	0.02	0.38
SERPINH1	0.46	0.25	1.00	0.66	0.08	1.00	-0.22	0.60	1.00	0.53	0.18	1.00	0.27	0.51	1.00
MRPL18	0.47	0.24	1.00	0.62	0.10	1.00	-0.03	0.94	1.00	0.50	0.21	1.00	0.55	0.15	1.00
RPA3	-0.17	0.7	1.00	-0.44	0.27	1.00	-0.35	0.39	1.00	-0.14	0.75	1.00	0.56	0.15	1.00
CRYAB	0.57	0.14	1.00	0.80	0.02	0.38	0.43	0.28	1.00	0.59	0.12	1.00	0.48	0.23	1.00
CAMK2A	0.33	0.18	1.00	0.69	0.06	1.00	0.61	0.11	1.00	0.45	0.26	1.00	0.66	0.07	1.00
CAMK2G	0.34	0.4	1.00	-0.03	0.95	1.00	0.45	0.26	1.00	0.71	0.05	0.95	0.81	0.02	0.38
MTOR	0.15	0.73	1.00	-0.17	0.69	1.00	-0.46	0.25	1.00	0.43	0.29	1.00	-0.03	0.94	1.00
HSPB8	0.15	0.73	1.00	0.06	0.89	1.00	0.30	0.47	1.00	0.65	0.08	1.00	-0.03	0.94	1.00

bioRxiv preprint doi: https://doi.org/10.1101/2024.12.06.627202; this version posted December 11, 2024. The copyright holder for this preprint (which was not certified by peer review) is the author/funder, who has granted bioRxiv a license to display the preprint in perpetuity. It is made available under aCC-BY-NC-ND 4.0 International license.

Supplemental Table 5. Summary of characteristics for the GWAS used in MAGMA

Shows the key characteristics and summary of statistics for the GWAS studies incorporated into our MAGMA analysis.

Phenotype	Citation	Groups Compared	Recruitment	Cohort Size	Age	Sex	Ethnicity	Genotype Method	Significant Loci (genes)
White Matter Hyperintensities (WMH)	https://doi.org/10.1038/s41467-020-19111-2	Quantitative Trait	CHARGE Consortium (24,182) & UK Biobank (26,788)	50,970	66.0 ± 7.5 y.o.	47% M / 53% F	European (>95% White)	Several	TRIM65, EFEMP1, NMT1, VCAN, NID2, KCNK2, ECHDC3, XKR6
Fractional Anisotropy (FA)	https://doi.org/10.1038/s41467-020-15932-3	Quantitative Trait	UK Biobank	17,663	63.3 ± 7.4 y.o.	47.3% M / 52.7% F	European (>94% White)	Applied Biosystems UK Biobank Axiom Array	VCAN, SPIRE2, TCF25, ZFP57, HBEGF, ICAL1, WDR12, CARF, NBEAL1
Small Vessel Stroke (SVS)	https://doi.org/10.1038/s41586-022-05165-3	Case Control	Meta-analysis of 29 cohorts	13,620	See supplemental Tables 1 and 2 in *Mishra et al 2022*			Several	PMF1, ZCCHC14, PRDM16, COL4A2, HTRA1, PTCH1
Enlarged Perivascular Spaces (PVS)	https://doi.org/10.1038/s41591-023-02268-w	Quantitative Trait	Meta-analysis of 18 cohorts	40,095	66.3 ± 8.6 y.o.	39% M / 61% F	European (>96% White)	Several	SLC13A3, WNT7A, ITGB5, GFAP, OPA1, EFEMP1, LPAR1, LAMC1
Alzheimer's Disease (AD)	https://doi.org/10.1038/s41588-022-01024-z	Case Control	Meta-analysis of 12 cohorts	487,511	See supplemental Tables 1 and 2 in *Bellenguez et al 2022*			Several	SORT1, ADAM17, NCK2, ICA1L, TNIP1, CTSB, TSPAN14, CTSH
Intracerebral Hemorrhage (ICH)	https://doi.org/10.1016/j.ajhg.2014.02.012	Case Control	Meta-analysis of 6 cohorts	6,968	See table 1 in *Woo et al 2014*			Several	TRHDE, PMF1, SLC25A44
Hair Color	https://doi.org/10.1038/s41588-021-00954-4	Case Control	UK Biobank	456,348	56.52 ± 8.09 y.o.	45.79% M / 54.21% F	European (>94% White)	Applied Biosystems UK Biobank Axiom Array	MCR1, ASIP, HERC2, OCA2, PKHD1, TSPAN10